

Magnetism of the antiferromagnetic spin- $\frac{3}{2}$ dimer compound CrVMoO₇ having an antiferromagnetically ordered state

Masashi Hase^{1,*}, Yuta Ebukuro², Haruhiko Kuroe², Masashige Matsumoto³, Akira Matsuo⁴, Koichi Kindo⁴, James R. Hester⁵, Taku J. Sato⁶, and Hiroki Yamazaki⁷

¹*Research Center for Advanced Measurement and Characterization,
National Institute for Materials Science (NIMS),
1-2-1 Sengen, Tsukuba-shi, Ibaraki 305-0047, Japan*

²*Department of Physics, Sophia University, 7-1 Kioi-cho, Chiyoda-ku, Tokyo 102-8554, Japan*

³*Department of Physics, Shizuoka University, 836 Ohya,
Suruga-ku, Shizuoka-shi, Shizuoka 422-8529, Japan*

⁴*The Institute for Solid State Physics (ISSP), The University of Tokyo,
5-1-5 Kashiwanoha, Kashiwa-shi, Chiba 277-8581, Japan*

⁵*Australian Centre for Neutron Scattering, Australian Nuclear Science and Technology Organisation (ANSTO),
Locked Bag 2001, Kirrawee DC NSW 2232, Australia*

⁶*Institute of Multidisciplinary Research for Advanced Materials (IMRAM),
Tohoku University, 2-1-1 Katahira, Aoba-ku, Sendai-shi, Miyagi 980-8577, Japan*

⁷*Nishina Center for Accelerator-Based Science, RIKEN,
2-1 Hirosawa, Wako-shi, Saitama 351-0198, Japan*

(Dated: February 17, 2017)

We measured magnetization, specific heat, electron spin resonance, neutron diffraction, and inelastic neutron scattering of CrVMoO₇ powder. An antiferromagnetically ordered state appears below $T_N = 26.5 \pm 0.8$ K. We consider that the probable spin model for CrVMoO₇ is an interacting antiferromagnetic spin- $\frac{3}{2}$ dimer model. We evaluated the intradimer interaction J to be 25 ± 1 K and the effective interdimer interaction J_{eff} to be 8.8 ± 1 K. CrVMoO₇ is a rare spin dimer compound that shows an antiferromagnetically ordered state at atmospheric pressure and zero magnetic field. The magnitude of ordered moments is $0.73(2)\mu_B$. It is much smaller than a classical value $\sim 3\mu_B$. Longitudinal-mode magnetic excitations may be observable in single crystalline CrVMoO₇.

PACS numbers: 75.25.-j, 75.30.Cr, 75.40.Cx, 75.30.Ds

I. INTRODUCTION

Two types of magnetic excitations exist in a magnetically ordered state. They are gapless transverse-mode (Nambu-Goldstone mode) [1] and gapped longitudinal-mode (Higgs mode) [2, 3] excitations corresponding to fluctuations in directions perpendicular and parallel to ordered moments, respectively. The transverse-mode (T-mode) excitations are well known as spin wave excitations. There are a few experimental observations on the longitudinal-mode (L-mode) excitations mainly because of their weak intensity. The L-mode excitations were observed in a pressure-induced or magnetic-field-induced magnetically ordered state of interacting antiferromagnetic (AF) spin- $\frac{1}{2}$ dimer compounds TlCuCl₃ [4–8] and KCuCl₃ [9]. The ground state (GS) is a spin-singlet state at atmospheric pressure and zero magnetic field in these compounds. The ordered state is in the vicinity of quantum phase transition. Therefore, the L-mode excitations are observable because of large quantum fluctuations.

According to results of theoretical investigations, the L-mode excitations may be observed in an antiferromagnetically ordered state appearing on cooling at atmospheric pressure and zero magnetic field in interacting

AF spin-cluster compounds [10]. A shrinkage of ordered magnetic moments by quantum fluctuations leads to a large intensity of the L-mode excitations. If the GS of the corresponding isolated spin cluster is a spin-singlet state, the shrinkage of ordered moments can be expected in an ordered state generated by the introduction of intercluster interactions.

In interacting spin clusters, the ordered state may appear under the condition that the value of an effective intercluster interaction is not so small compared with that of Δ [10]. Here the effective intercluster interaction is given by the sum of the products of the absolute value of each intercluster interaction ($|J_{\text{int},i}|$) and the corresponding number of interactions per spin (z_i) as $J_{\text{eff}} = \sum_i z_i |J_{\text{int},i}|$. Δ is the energy difference (spin gap) between the singlet GS and first-excited triplet states. It is advantageous for the appearance of the ordered state that Δ is much smaller than the dominant intracluster interactions. In a spin- $\frac{1}{2}$ tetramer of which the Hamiltonian $\mathcal{H} = J_1 S_2 \cdot S_3 + J_2 (S_1 \cdot S_2 + S_3 \cdot S_4)$ with $J_1 > 0$ and $J_2 < 0$, the GS is a spin-singlet state and Δ/J_1 can be sufficiently small [11–13]. The values of J_1 , J_2 , J_{eff} , and Δ are 317, -162, 42, and 19 K, respectively, in Cu₂CdB₂O₆ [14] and 240, -142, 30, and 17 K, respectively, in CuInVO₅ [13]. The ordered state appears in Cu₂CdB₂O₆ [12, 14, 15] and CuInVO₅ [13] below the transition temperature $T_N = 9.8$ and 2.7 K, respectively. Magnetic excitations in Cu₂¹¹⁴Cd¹¹B₂O₆ were studied by

*Electronic address: HASE.Masashi@nims.go.jp

inelastic neutron scattering experiments on its powder [14]. The results suggest the existence of the L-mode excitations. Magnetic excitations in CuInVO_5 have not been investigated.

Spin dimer compounds are also attractive for investigation of the L-mode excitations at atmospheric pressure and zero magnetic field. In contrast with the small Δ/J_1 in the spin- $\frac{1}{2}$ tetramer, the value of Δ/J is 1 in the isolated AF spin dimer given by $JS_1 \cdot S_2$ irrespective of the spin value. It is rare that spin dimer compounds show a magnetically ordered state at atmospheric pressure and zero magnetic field. An example is the AF spin- $\frac{1}{2}$ dimer compound NH_4CuCl_3 [16–18].

We can expect an interacting AF spin- $\frac{3}{2}$ dimer model in CrVMoO_7 from its crystal structure as shown in Fig. 1(a) [19, 20]. Only the Cr^{3+} ion ($3d^3$) has a localized spin- $\frac{3}{2}$. The shortest distance between two Cr^{3+} ions is 3.01 Å at 153 K, whereas the other Cr-Cr distances are larger than 4.96 Å [19]. We found an antiferromagnetically ordered state below $T_N = 26.5 \pm 0.8$ K. We investigated magnetism of CrVMoO_7 using magnetization, specific heat, electron spin resonance, neutron diffraction, and inelastic neutron scattering experiments. In this paper, we report the results.

II. EXPERIMENTAL AND CALCULATION METHODS

Crystalline CrVMoO_7 powder was synthesized by a solid-state reaction. Starting materials are Cr_2O_3 , V_2O_5 , and MoO_3 powder. Their purity is 99.99 %. A stoichiometric mixture of powder was sintered at 923 K in air for 268 h with intermediate grindings. We measured an x-ray powder diffraction pattern at room temperature using an x-ray diffractometer (RINT-TTR III, Rigaku). We confirmed that our sample was a nearly single phase of CrVMoO_7 .

Electron spin resonance (ESR) measurements were performed using an X-band spectrometer (JES-RE3X, JEOL) at room temperature. We measured the specific heat using a physical property measurement system (Quantum Design). We measured the magnetization in magnetic fields of up to 5 T using a superconducting quantum interference device magnetometer magnetic property measurement system (Quantum Design). High-field magnetization measurements were conducted using an induction method with a multilayer pulsed field magnet installed at the Institute for Solid State Physics (ISSP), the University of Tokyo.

We carried out neutron powder diffraction experiments using the high-intensity powder diffractometer Wombat (Proposal ID P5174) at Australia's Open Pool Australian Lightwater (OPAL) reactor in Australian Centre for Neutron Scattering in Australian Nuclear Science and Technology Organisation (ANSTO). We performed Rietveld refinements of the crystal and magnetic structures using the FULLPROF SUITE program package [21] with its

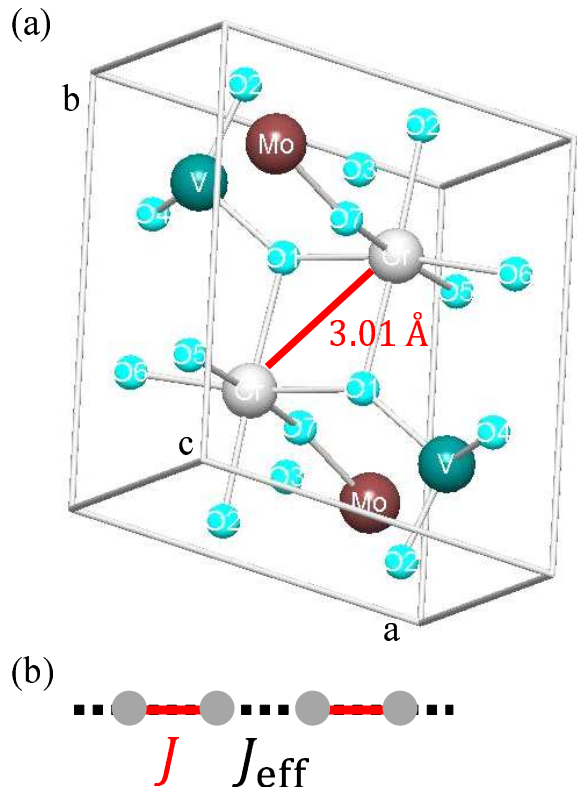


FIG. 1: (Color online) (a) The unit cell of CrVMoO_7 [19, 20]. An AF spin- $\frac{3}{2}$ dimer is formed by two neighboring Cr^{3+} ions ($3d^3$ electron configuration) with the distance of 3.01 Å. (b) Interacting spin dimer model used to calculate magnetization using a mean-field theory based on the dimer unit (dimer mean-field theory).

internal tables for scattering lengths and magnetic form factors. We performed inelastic neutron scattering (INS) measurements using the inverted geometry time-of-flight spectrometer LAM-40 in High Energy Accelerator Research Organization (KEK).

We obtained the eigenenergies of isolated spin- $\frac{3}{2}$ dimers using an exact diagonalization method. We calculated the temperature T dependence of the magnetic susceptibility $\chi(T)$ and the magnetic-field H dependence of the magnetization $M(H)$ using the eigenenergies.

We calculated $M(H)$ for the model shown in Fig. 1(b) using a mean-field theory based on the dimer unit (dimer mean-field theory). Finite magnetic moments were initially assumed on the Cr sites in the dimer. The mean-field Hamiltonian was then expressed by a 16×16 matrix form under consideration of the external magnetic field and the molecular field from the nearest neighbor sites. The eigenstates of the mean-field Hamiltonian were used to calculate the expectation value of the ordered moments on the Cr sites. We continued this procedure until the values of the magnetic moments converged. We finally obtained a self-consistently determined solution for

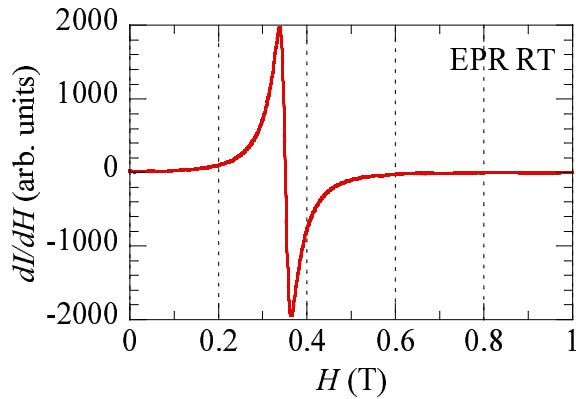


FIG. 2: (Color online) The electron paramagnetic resonance (EPR) spectrum of a CrVMoO₇ pellet at room temperature measured using an X-band electron spin resonance (ESR).

$M(H)$.

III. RESULTS AND DISCUSSION

Figure 2 shows the H derivative of the intensity of electron paramagnetic resonance (EPR) of a CrVMoO₇ pellet at room temperature. The frequency of the incident microwave is 9.455 GHz. A clear resonance appeared. We evaluated the g value to be 1.92 ± 0.02 .

Figure 3(a) shows the T dependence of the specific heat $C(T)$ of CrVMoO₇ in zero magnetic field and the T derivative of the magnetic susceptibility $\chi(T)$ of CrVMoO₇ in $H = 0.1$ T. The sample was a pressed pellet and powder for $C(T)$ and $\chi(T)$, respectively. We can see a peak around 26.5 K in $C(T)$ and around 25.5 K in $d\chi(T)/dT$. As described later, we observed an antiferromagnetically ordered state at low T in neutron powder diffraction experiments. The peak indicates the phase transition. We determined the transition temperature $T_N = 26.5 \pm 0.8$ K mainly from the specific heat result.

The red circles in Fig. 3(b) show the T dependence of $\chi(T)$ of CrVMoO₇ powder in $H = 0.1$ T. The broad maximum of $\chi(T)$ around 35 K indicates a low-dimensional AF spin system. The susceptibility seems to approach a finite value (~ 0.012 emu/mol Cr) at 0 K. The magnetic order results in the probable finite susceptibility at 0 K. The susceptibility obtained by us is close to that reported in literature [19, 22].

We considered the simple isolated AF spin- $\frac{3}{2}$ dimer model as a first approximation because of the following reasons. The spin- $\frac{3}{2}$ on Cr³⁺ ions is usually a Heisenberg spin. The Cr³⁺ ion is coordinated octahedrally by six oxygen ions. Symmetries of crystal fields affecting the Cr³⁺ ions are nearly cubic. It is inferred that single ion anisotropy of the Cr³⁺ ions is small. The green line in Fig. 3(b) shows $\chi(T)$ calculated for the isolated AF spin- $\frac{3}{2}$ dimer with $J = 25$ K and $g = 1.92$ that was determined

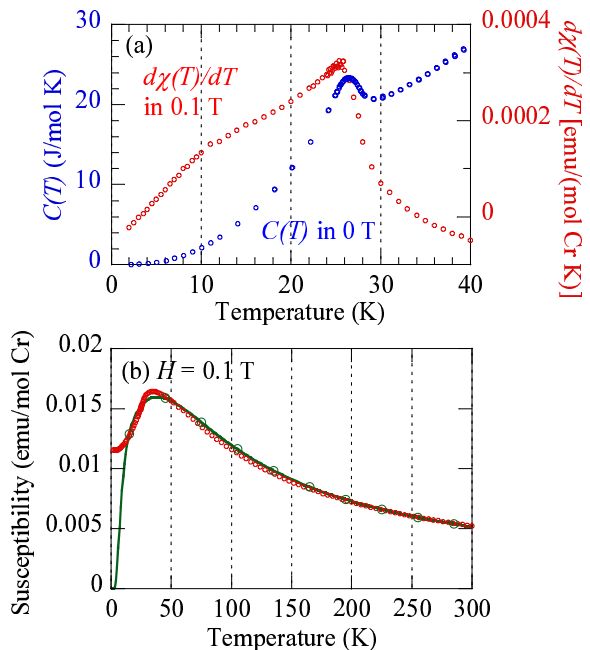


FIG. 3: (Color online) (a) Temperature T dependence of the specific heat $C(T)$ of CrVMoO₇ in zero magnetic field and T derivative of the magnetic susceptibility $\chi(T)$ of CrVMoO₇ in a magnetic field of $H = 0.1$ T. (b) T dependence of $\chi(T)$ of CrVMoO₇ in $H = 0.1$ T (red circles). A green line with several circles indicates $\chi(T)$ calculated for an isolated AF spin- $\frac{3}{2}$ dimer with $J = 25$ K and $g = 1.92$.

in EPR. The experimental and calculated $\chi(T)$ are close to each other at high T . We evaluated J to be 25 ± 1 K.

An exchange interaction between two $\frac{3}{2}$ spins localized on magnetic ions with the $3d^3$ electron configuration is dominated by an AF direct exchange interaction. Therefore, the magnitude of the exchange interaction J_{3d^3} is mainly determined by the distance R between two magnetic ions. There is an empirical relation $J_{3d^3} = a \exp(-R/b)$ with $a = 8.7 \times 10^7$ K and $b = 0.21$ Å for compounds including Cr³⁺ ions ($3d^3$) [23]. The value of J_{3d^3} was calculated to be 53 K for $R = 3.01$ Å. The values of J and J_{3d^3} are the same in order.

The red lines in Fig. 4 show the H dependence of the magnetization $M(H)$ of CrVMoO₇ powder measured at 1.3 and 30 K. The magnetization increases monotonically with increase in H . The green lines in Fig. 4 indicate $M(H)$ calculated for the isolated AF spin- $\frac{3}{2}$ dimer with $J = 25$ K and $g = 1.92$. The calculated $M(H)$ is close to the experimental $M(H)$ at 30 K, whereas the isolated spin dimer model fails to reproduce the experimental $M(H)$ at 1.3 K. There are $\frac{1}{3}$ and $\frac{2}{3}$ quantum magnetization plateaus in the calculated line, whereas no plateau exists in the experimental line. The $\frac{1}{3}$ and $\frac{2}{3}$ magnetization-plateau phases are polarized paramagnetic phases in which $S^T = 1$ and 2, respectively. Here S^T represents the size of the total spin of the two $S = \frac{3}{2}$

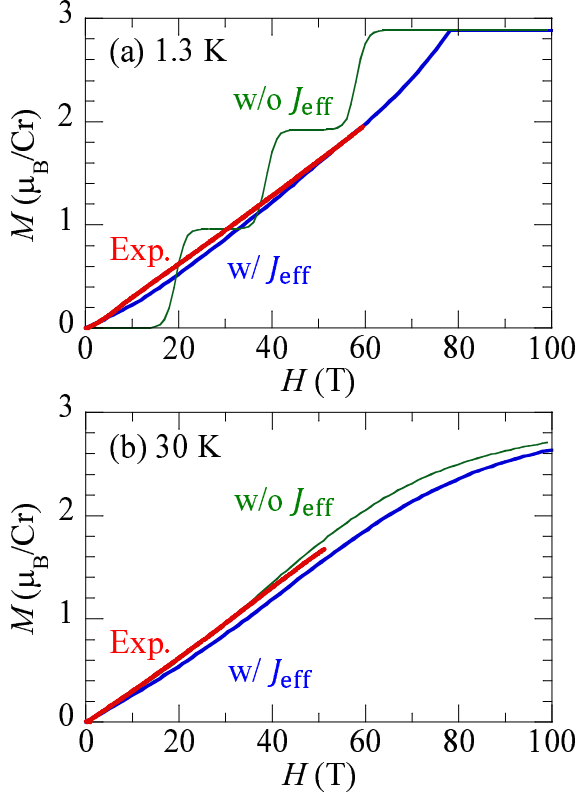


FIG. 4: (Color online) Magnetic-field H dependence of the magnetization $M(H)$ of CrVMoO_7 powder (red lines). Blue and green lines indicate $M(H)$ calculated for the interacting spin- $\frac{3}{2}$ dimer model in Fig. 1(b) labeled by w/ J_{eff} and for an isolated spin- $\frac{3}{2}$ dimer labeled by w/o J_{eff} , respectively. The values of the parameters are $J = 25$ K, $J_{\text{eff}} = 8.8$ K, and $g = 1.92$. (a) $M(H)$ at 1.3 K. (b) $M(H)$ at 30 K.

spins. We could not find the J value of the isolated spin dimer model that reproduced the experimental $M(H)$ at 1.3 K.

According to the results in CuInVO_5 [13], the discrepancy between experimental and calculated $M(H)$ is probably caused by interdimer interactions. Interdimer interactions must exist in CrVMoO_7 to stabilize the ordered state. Interdimer interactions have a greater effect on the magnetization at lower T . Therefore, the discrepancy between the experimental results and those calculated for the isolated spin dimer appears at low T . We assumed the simple model shown in Fig. 1(b) as in the case of CuInVO_5 [13] and calculated $M(H)$ using the dimer mean-field theory. The blue lines in Fig. 4 indicate $M(H)$ calculated for the interacting spin dimer model with $J = 25$ K, $J_{\text{eff}} = 8.8$ K, and $g = 1.92$. The experimental and calculated $M(H)$ are in agreement with each other. The J_{eff} value is not so small compared with the J value. Therefore, the antiferromagnetically ordered state appears.

We can explain qualitatively $M(H)$ of CrVMoO_7 . In

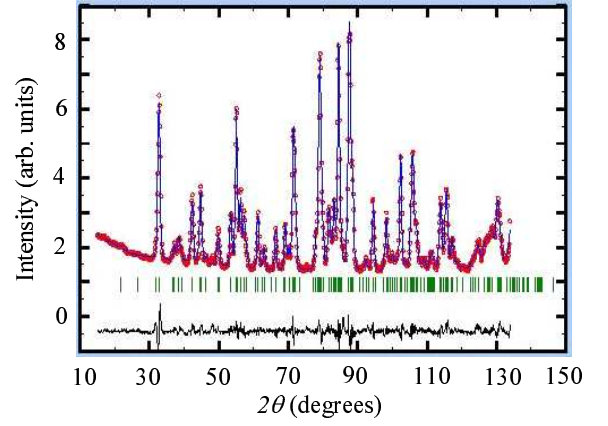


FIG. 5: (Color online) A neutron powder diffraction pattern (circles) of CrVMoO_7 at 35 K. The wavelength λ is 2.955 Å. A blue line on the measured pattern portrays a Rietveld refined pattern obtained using the crystal structure with $P-1$ (No. 2). A line at the bottom portrays the difference between the measured and the Rietveld refined patterns. Hash marks represent positions of nuclear reflections.

a weakly interacting spin dimer model, magnetization plateaus exist at low T . Magnetization-plateau phases are polarized paramagnetic phases without a spontaneous magnetic order. An ordered phase can appear in a magnetic-field range, where $M(H)$ increases, between two magnetization-plateau phases. In the case of spin- $\frac{3}{2}$, there are three types of ordered phases, phase 1, 2, and 3 at $0 \leq H < H_{1s}$, $H_{1f} < H < H_{2s}$, and $H_{2f} < H < H_{3s}$, respectively. Here, H_{is} and H_{if} indicate magnetic fields at which the $\frac{1}{3}$ plateau starts and finishes, respectively. The phase 1 is mainly formed by $S^T = 0$ and $S^T = 1$ states of isolated AF spin dimers. The phase 2 is mainly formed by $S^T = 1$ and $S^T = 2$ states. The phase 3 is mainly formed by $S^T = 2$ and $S^T = 3$ states. As interdimer interactions increase, magnetic-field ranges of ordered phases are spread. When interdimer interactions are strong, the ordered phases are connected with each other. A single ordered phase is formed until the saturation of the magnetization. Therefore, the magnetization increases monotonically with increase in H .

The circles in Fig. 5 show a neutron powder diffraction pattern of CrVMoO_7 at 35 K above $T_N = 26.5 \pm 0.8$ K. The wavelength λ is 2.955 Å. We performed Rietveld refinements using the space group $P-1$ (No. 2) to evaluate crystal structure parameters. The line on the experimental pattern indicates the result of Rietveld refinements. The line agrees with the experimental pattern. The refined crystal structure parameters are presented in Table I. The atomic positions in our results are similar to those in the literature [19, 20].

Figure 6(a) shows neutron powder diffraction patterns of CrVMoO_7 at 5 and 35 K. The two patterns nearly overlap each other except for around $2\theta = 20^\circ$. Figure 6(b) shows the difference pattern made by subtracting

TABLE I: Structural parameters of CrVMoO₇ derived from Rietveld refinements of the neutron powder diffraction pattern at 35 K. We used triclinic $P-1$ (No. 2). The lattice constants are $a = 5.521(1)$ Å, $b = 6.575(1)$ Å, $c = 7.859(1)$ Å, $\alpha = 96.24(1)^\circ$, $\beta = 89.91(1)^\circ$, and $\gamma = 101.99(1)^\circ$. Estimated standard deviations are shown in parentheses. The reliability indexes of the refinement are $R_p = 3.16$ %, $R_{wp} = 4.14$ %, and $R_{exp} = 0.21$ %.

Atom	Site	x	y	z	B_{iso} Å ²
Cr	$2i$	0.826(3)	0.310(3)	0.408(2)	0.30(4)
V	$2i$	0.311(3)	0.242(3)	0.665(3)	0.31(5)
Mo	$2i$	0.301(2)	0.209(1)	0.109(1)	0.24(5)
O1	$2i$	0.203(2)	0.981(1)	0.616(1)	0.33(5)
O2	$2i$	0.108(3)	0.375(1)	0.574(1)	0.33(5)
O3	$2i$	0.336(2)	0.295(2)	0.891(1)	0.33(5)
O4	$2i$	0.597(2)	0.314(1)	0.580(1)	0.33(5)
O5	$2i$	0.057(2)	0.319(1)	0.222(1)	0.33(5)
O6	$2i$	0.564(2)	0.292(1)	0.233(1)	0.33(5)
O7	$2i$	0.213(2)	0.948(2)	0.098(1)	0.33(5)

the neutron powder diffraction pattern at 35 K from that at 5 K. Several magnetic reflections are apparent at 5 K. All the reflections can be indexed with the propagation vector $\mathbf{k} = (\frac{1}{2}, 0, \frac{1}{2})$.

The inset in Fig. 6(b) shows the T dependence of the integrated intensity between 17 and 22° including $-\frac{1}{2}0\frac{1}{2}$ and $\frac{1}{2}0\frac{1}{2}$ reflections. The intensity increases with decrease in T and is nearly constant below 14 K. The blue line indicates $A(1 - \frac{T}{T_N})^{2\beta}$ with $A = 1.98$, $T_N = 27.3$ K, and $\beta = 0.29$. These values were obtained from the data above 20 K. We evaluated β to be 0.26 in the spin- $\frac{1}{2}$ tetramer compound Cu₂CdB₂O₆ from the inset figure in Fig. 4 in [12]. The two values of the critical exponent are close to each other. The β value is 0.36, 0.33, and 1/8 for three-dimensional Heisenberg, three-dimensional Ising, and two-dimensional Ising models, respectively. In the Ising models, β is smaller in the lower dimension. The spin models in CrVMoO₇ and Cu₂CdB₂O₆ are low-dimensional AF interacting spin clusters. Therefore, the β values in these compounds are smaller than that of three-dimensional Heisenberg models.

According to magnetic space groups in $P-1$ [24], only a collinear magnetic structure is possible. We performed Rietveld refinements for the difference pattern using two models. Two ordered moments in each dimer are parallel in one model and antiparallel in the other one. As expected, only the antiparallel model can explain the magnetic reflections as shown in Fig. 6(b).

The magnetic structure is shown in Fig. 7 [25]. An ordered moment vector is $(0.02(2), 0.60(1), -0.36(2))\mu_B$ lying nearly in the bc plane. Its magnitude is $0.73(2)\mu_B$. It is much smaller than a classical value $\sim 3\mu_B$. The GS of the spin dimer is a spin-singlet state [26–28]. Therefore, the ordered moment is shrunk.

Figure 8 shows INS intensity $I(Q, \omega)$ maps of CrVMoO₇ powder at 1.5 and 30 K. Here, Q and ω are the magnitude of the scattering vector and the energy transfer, respectively. The energy of final neutrons E_f is 4.59 meV. We can see excitations between 2 and 7 meV at 1.5 K. The intensity of the excitations is suppressed at higher Q . Excitations at 1.5 K also exist below 2 meV

around $Q = 0.7$ Å⁻¹. Excitations at 30 K exist in lower energies in comparison with those at 1.5 K. The intensity is strong at low ω around $Q = 0.7$ Å⁻¹.

Figure 9(a) shows the ω dependence of $I(Q, \omega)$ in the Q range of $0.95 - 1.05$ Å⁻¹. The intensity at 1.5 K is the strongest around 4.5 meV. The intensity at 30 K decreases with increase in ω . The red circles in Fig. 9(b) show the Q dependence of $I(Q, \omega)$ at 1.5 K summed in the ω range of 4 - 5 meV. The intensity shows a peak around $Q = 1.0$ Å⁻¹.

Considering the INS results of Cu₂CdB₂O₆ [14], we can explain qualitatively the INS results of CrVMoO₇ using the interacting AF spin- $\frac{3}{2}$ dimer model. The blue line in Fig. 9(b) indicates the Q dependence of the intensity calculated for the isolated spin dimer model with the Cr-Cr distance of 3.01 Å. The experimental and calculated results are similar to each other. The first excited spin-triplet states exist at 2.2 meV (= 25 K) in the isolated AF spin- $\frac{3}{2}$ dimer. Interdimer interactions change discrete levels of excited states to excitation bands with finite widths. The excitations between 2 and 7 meV indicate the existence of the excitation bands [29].

The magnetic reflection is the strongest at $-\frac{1}{2}0\frac{1}{2}$. The magnetic zone center of the spin configuration shown in Fig. 7 is $-\frac{1}{2}0\frac{1}{2}$. The Q value is 0.70 Å⁻¹. Therefore, the excitations at 1.5 K below 2 meV around $Q = 0.7$ Å⁻¹ are T-mode (Nambu-Goldstone mode) excitations in the vicinity of the gapless point.

The magnetic excitations are gapless below T_N . The temperature 30 K is slightly higher than $T_N = 26.5 \pm 0.8$ K. The bandwidths are large and the excitation gap is small. Therefore, magnetic excitations appear in low energies. Excitations from thermally excited states in the excitation bands also generate the continuous low-energy intensities at 30 K.

We could not confirm L-mode excitations because of the powder sample. We intend to make single crystals of CrVMoO₇ and to perform INS and Raman scattering experiments on them to investigate L-mode excitations. We expect that L-mode excitations are observable because of the small ordered moment.

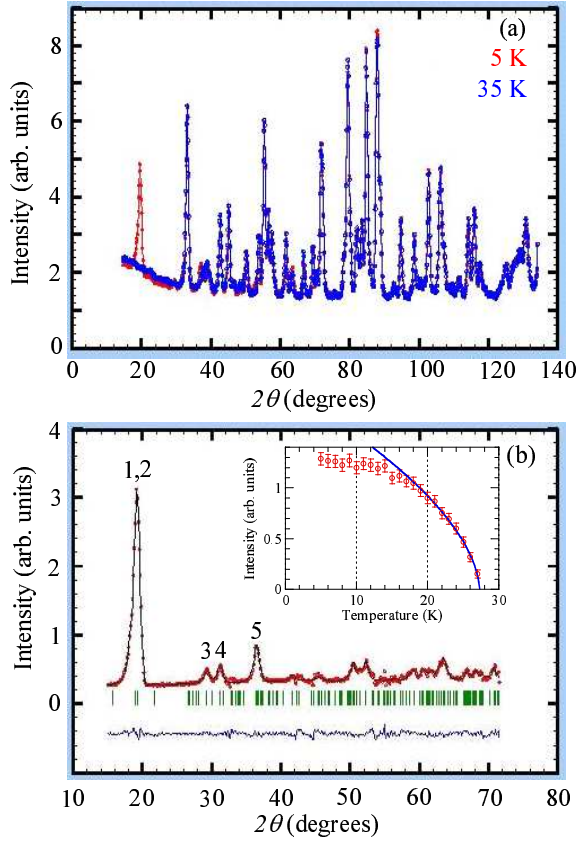


FIG. 6: (Color online) (a) Neutron powder diffraction patterns of CrVMoO₇ at 5 and 35 K. The wavelength λ is 2.955 Å. (b) A difference pattern made by subtracting a neutron powder diffraction pattern at 35 K from that at 5 K. A line on the measured pattern portrays a Rietveld refined pattern of the magnetic structure. A line at the bottom portrays the difference between the measured and the Rietveld refined patterns. Hash marks represent positions of magnetic reflections. The reliability indexes of the refinement are $R_p = 4.37\%$, $R_{wp} = 6.17\%$, and $R_{exp} = 0.46\%$. Indexes of major magnetic reflections labeled by 1, 2, 3, 4, and 5 are $-\frac{1}{2}0\frac{1}{2}$, $\frac{1}{2}0\frac{1}{2}$, $\frac{1}{2} - 1\frac{1}{2}$, $-\frac{1}{2}1\frac{1}{2}$, and $-\frac{1}{2}0\frac{3}{2}$, respectively. The inset shows T dependence of the integrated intensity between 17 and 22°. A blue line indicates $A(1 - \frac{T}{T_N})^{2\beta}$ with $A = 1.98$, $T_N = 27.3$ K, and $\beta = 0.29$.

IV. CONCLUSION

We investigated magnetism of CrVMoO₇ using magnetization, specific heat, electron spin resonance, neutron diffraction, and inelastic neutron scattering experiments. An antiferromagnetically ordered state appears below $T_N = 26.5 \pm 0.8$ K. The magnetic susceptibility of CrVMoO₇ powder at high T is close to that calculated for the isolated AF spin- $\frac{3}{2}$ dimer with the intradimer interaction value $J = 25 \pm 1$ K and $g = 1.92 \pm 0.02$. We were able to explain the magnetization curves using the interacting AF spin- $\frac{3}{2}$ dimer model with the effective in-

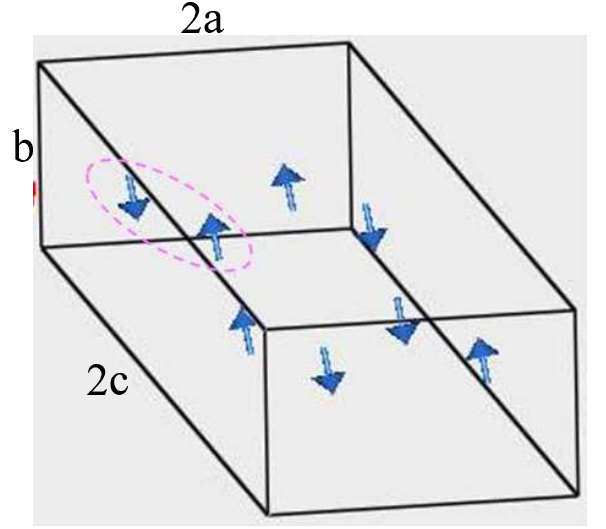


FIG. 7: (Color online) The magnetic structure of CrVMoO₇. An ellipse indicates an AF dimer.

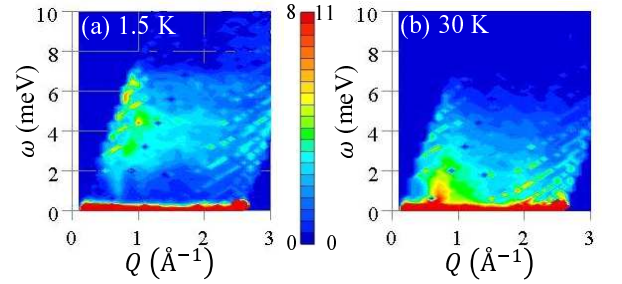


FIG. 8: (Color online) INS intensity $I(Q, \omega)$ maps in the $Q - \omega$ plane for CrVMoO₇ powder at 1.5 K (a) and 30 K (b) measured using the LAM-40 spectrometer. The energy of final neutrons E_f is 4.59 meV. The right vertical key shows the INS intensity in arbitrary units.

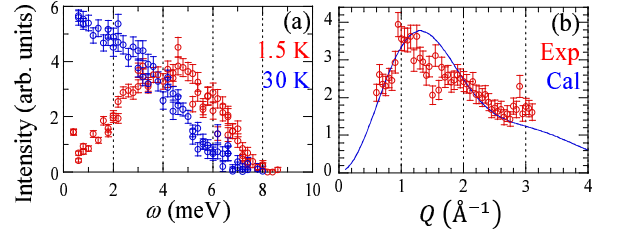


FIG. 9: (Color online) (a) ω dependence of the INS intensity for CrVMoO₇ powder in the Q range of $0.95 - 1.05$ Å⁻¹ at 1.5 and 30 K. (b) The Q dependence of the INS intensity of CrVMoO₇ powder summed in the ω range of 4 - 5 meV at 1.5 K (circles). A line indicates the intensity calculated for an isolated AF spin- $\frac{3}{2}$ dimer. The formula is $Af(Q)^2[1 - \sin(3.01Q)/(3.01Q)]$ where A and $f(Q)$ represent a scaling factor and an atomic magnetic form factor, respectively.

terdimer interaction $J_{\text{eff}} = 8.8 \pm 1$ K. We determined the magnetic structure of CrVMoO_7 . The magnitude of ordered moments is $0.73(2)\mu_B$. It is much smaller than a classical value $\sim 3\mu_B$. Two ordered moments are antiparallel in each dimer. We observed magnetic excitations in inelastic neutron scattering experiments. We can explain qualitatively the results using the interacting AF spin- $\frac{3}{2}$ dimer model. CrVMoO_7 is a rare spin dimer compound that shows an antiferromagnetically ordered state at atmospheric pressure and zero magnetic field. Longitudinal-mode magnetic excitations may be observable in single crystalline CrVMoO_7 .

Acknowledgments

This work was financially supported by Japan Society for the Promotion of Science (JSPS) KAKENHI (Grant

No. 15K05150) and grants from National Institute for Materials Science (NIMS). M. M. was supported by JSPS KAKENHI (Grant No. 26400332). The high-field magnetization experiments were conducted under the Visiting Researcher's Program of the Institute for Solid State Physics (ISSP), the University of Tokyo. The neutron powder diffraction experiments were performed by using the Wombat diffractometer at Australian Nuclear Science and Technology Organisation (ANSTO), Australia (proposal ID. P5174). We are grateful to S. Matsumoto for sample syntheses and x-ray diffraction measurements.

-
- [1] J. Goldstone, A. Salam, and S. Weinberg, Broken Symmetries, *Phys. Rev.* **127**, 965 (1962).
 - [2] S. Sachdev, *Quantum Phase Transitions* Second Edition (Cambridge University Press, Cambridge, U.K., 2011).
 - [3] D. Podolsky, A. Auerbach, and D. P. Arovas, Visibility of the amplitude (Higgs) mode in condensed matter, *Phys. Rev. B* **84**, 174522 (2011).
 - [4] H. Kuroe, K. Kusakabe, A. Oosawa, T. Sekine, F. Yamada, H. Tanaka, and M. Matsumoto, Magnetic field-induced one-magnon Raman scattering in the magnon Bose-Einstein condensation phase of TiCuCl_3 , *Phys. Rev. B* **77**, 134420 (2008).
 - [5] Ch. Rüegg, B. Normand, M. Matsumoto, A. Furrer, D. F. McMorrow, K. W. Krämer, H.-U. Güdel, S. N. Gvasaliya, H. Mutka, and M. Boehm, Quantum Magnets under Pressure: Controlling Elementary Excitations in TiCuCl_3 , *Phys. Rev. Lett.* **100**, 205701 (2008).
 - [6] P. Merchant, B. Normand, K. W. Krämer, M. Boehm, D. F. McMorrow, and Ch. Rüegg, Quantum and classical criticality in a dimerized quantum antiferromagnet, *Nat. Phys.* **10**, 373 (2014).
 - [7] M. Matsumoto, B. Normand, T. M. Rice, and M. Sigrist, Field- and pressure-induced magnetic quantum phase transitions in TiCuCl_3 , *Phys. Rev. B* **69**, 054423 (2004).
 - [8] M. Matsumoto, H. Kuroe, A. Oosawa, and T. Sekine, One-Magnon Raman Scattering as a Probe of Longitudinal Excitation Mode in Spin Dimer Systems, *J. Phys. Soc. Jpn.* **77**, 033702 (2008).
 - [9] H. Kuroe, N. Takami, N. Niwa, T. Sekine, M. Matsumoto, F. Yamada, H. Tanaka, and K. Takemura, Longitudinal magnetic excitation in KCuCl_3 studied by Raman scattering under hydrostatic pressures, *J. Phys.: Conf. Ser.* **400**, 032042 (2012).
 - [10] M. Matsumoto, H. Kuroe, T. Sekine, and T. Masuda, Transverse and Longitudinal Excitation Modes in Interacting Multispin Systems, *J. Phys. Soc. Jpn.* **79**, 084703 (2010).
 - [11] M. Hase, K. M. S. Etheredge, S.-J. Hwu, K. Hirota, and G. Shirane, Spin-singlet ground state with energy gaps in Cu_2PO_4 : Neutron-scattering, magnetic-susceptibility, and ESR measurements, *Phys. Rev. B* **56**, 3231 (1997). In this reference, the Hamiltonian is defined as $\mathcal{H} = \sum_{i,j} 2J_{ij} S_i \cdot S_j$ instead of $\mathcal{H} = \sum_{i,j} J_{ij} S_i \cdot S_j$ in the present paper.
 - [12] M. Hase, A. Dönni, V. Yu. Pomjakushin, L. Keller, F. Gozzo, A. Cervellino, and M. Kohno, Magnetic structure of $\text{Cu}_2\text{CdB}_2\text{O}_6$ exhibiting a quantum-mechanical magnetization plateau and classical antiferromagnetic long-range order, *Phys. Rev. B* **80**, 104405 (2009).
 - [13] M. Hase, M. Matsumoto, A. Matsuo, and K. Kindo, Magnetism of the antiferromagnetic spin- $\frac{1}{2}$ tetramer compound CuInVO_5 , *Phys. Rev. B* **94**, 174421 (2016).
 - [14] M. Hase, K. Nakajima, S. Ohira-Kawamura, Y. Kawakita, T. Kikuchi, and M. Matsumoto, Magnetic excitations in the spin- $\frac{1}{2}$ tetramer substance $\text{Cu}_2^{114}\text{Cd}^{11}\text{B}_2\text{O}_6$ obtained by inelastic neutron scattering experiments, *Phys. Rev. B* **92**, 184412 (2015).
 - [15] M. Hase, M. Kohno, H. Kitazawa, O. Suzuki, K. Ozawa, G. Kido, M. Imai, and X. Hu, Coexistence of a nearly spin-singlet state and antiferromagnetic long-range order in quantum spin system $\text{Cu}_2\text{CdB}_2\text{O}_6$, *Phys. Rev. B* **72**, 172412 (2005).
 - [16] B. Kurniawan, M. Ishikawa, T. Kato, H. Tanaka, K. Takizawa, and T. Goto, Novel three-dimensional magnetic ordering in the quantum spin system NH_4CuCl_3 , *J. Phys.: Condens. Matter* **11**, 9073 (1999).
 - [17] M. Matsumoto, Theoretical Study of Magnetic Excitation in Interacting Inequivalent Spin Dimer System NH_4CuCl_3 , *J. Phys. Soc. Jpn.* **84**, 034701 (2015).
 - [18] B. Leuenberger, H. U. Güdel, and P. Fischer, Spontaneous Magnetic Order Induced by an Intratriplet Mode in the Dimerized Singlet-Ground-State System $\text{Cs}_3\text{Cr}_2\text{I}_9$, *Phys. Rev. Lett.* **55**, 2983 (1985). The intradimer interaction in $\text{Cs}_3\text{Cr}_2\text{I}_9$ was considered to be AF. Two ordered magnetic moments in each dimer, however, are parallel to each other. The result seems to suggest a ferromagnetic intradimer interaction. In the temperature dependence of the magnetic susceptibility, there is no broad maximum that is usually seen in low-dimensional antiferromagnets.
 - [19] X. Wang, K. R. Heier, C. L. Stern, and K. R. Poepe-

- pelmeier, Crystal structure and Raman spectroscopy of FeVMoO_7 and CrVMoO_7 with $\text{Mo}=\text{O}$ double bonds, *Inorg. Chem.* **37**, 3252 (1998).
- [20] K. Knorr, P. Jakubus, J. Walczak, and E. Filipek, The structure of CrVMoO_7 , *Eur. J. Solid State Inorg. Chem.* **35**, 161 (1998).
- [21] J. Rodriguez-Carvajal, Recent advances in magnetic structure determination by neutron powder diffraction, *Physica B* **192**, 55 (1993); [<http://www.ill.eu/sites/fullprof/>].
- [22] I. L. Botto, M. B. Vassallo, and R. S. Puche, Magnetic and spectroscopic properties of the CrVMoO_7 phase, *Anales de la Asociación Química Argentina* **86**, 29 (1998).
- [23] M. Hase, M. Soda, T. Masuda, D. Kawana, T. Yokoo, S. Itoh, A. Matsuo, K. Kindo, and M. Kohno, Experimental confirmation of spin gap in antiferromagnetic alternating spin- $\frac{3}{2}$ chain substances $R\text{CrGeO}_5$ ($R = \text{Y}$ or ^{154}Sm) by inelastic neutron scattering experiments, *Phys. Rev B* **90**, 024416 (2014).
- [24] D. B. Litvin, Tables of crystallographic properties of magnetic space groups, *Acta Crystallogr. A* **64**, 419 (2008).
- [25] Strictly speaking, the unit cell vectors of the magnetic structure are $\vec{a} + \vec{c}$, \vec{b} , and $\vec{a} - \vec{c}$. The unit cell of the magnetic structure is the double of that of the crystal structure.
- [26] M. Hase, I. Terasaki, and K. Uchinokura, Observation of the Spin-Peierls Transition in Linear Cu^{2+} (Spin- $\frac{1}{2}$) Chains in an Inorganic Compound CuGeO_3 , *Phys. Rev. Lett.* **70**, 3651 (1993).
- [27] M. Hase, I. Terasaki, Y. Sasago, K. Uchinokura, and H. Obara, Effects of Substitution of Zn for Cu in the Spin-Peierls Cuprate, CuGeO_3 : The Suppression of the Spin-Peierls Transition and the Occurrence of a New Spin-Glass State, *Phys. Rev. Lett.* **71**, 4059 (1993).
- [28] M. Hase, I. Terasaki, K. Uchinokura, M. Tokunaga, N. Miura, and H. Obara, Magnetic phase diagram of the spin-Peierls cuprate CuGeO_3 , *Phys. Rev. B* **48**, 9616 (1993).
- [29] In the spin- $\frac{1}{2}$ tetramer compound $\text{Cu}_2\text{CdB}_2\text{O}_6$ [14], the first excited spin-triplet states exist at 1.6 meV in the isolated tetramer. Magnetic excitations are spread between 1.6 and 3.0 meV by intertetramer interactions.